Journal of Applied Polymer Science

Synergistic effect of dipentaerythritol and montmorillonite in EVOH-based nanocomposites

Micaela Vannini,[1] Paola Marchese,[1] Annamaria Celli,[1] Carla Marega,[2] Antonio Marigo,[2] Cesare Lorenzetti[3]

[1]Dipartimento di Ingegneria Civile, Chimica, Ambientale e dei Materiali, Via Terracini 28, Bologna 40131, Italy
[2]Dipartimento di Scienze Chimiche, Università di Padova, Via Marzolo, 1, Padova 35131, Italy
[3]Tetra Pak SA, Zone Industrielle la Maillarde 2, Romont 1680, Switzerland
Correspondence to: A. Celli (E-mail: annamaria.celli@unibo.it)

ABSTRACT: To solve problems of stiffness of EVOH in film preparation, new formulations are investigated. First, dipentaerythritol (DPE) is blended with EVOH: it acts as plasticizer, decreases the EVOH crystallization temperature and allows the preparation of articles featuring enhanced flexibility and stretchability. However, beyond a certain loading (above 10 wt %) DPE can crystallize and segregate during cooling, causing further problems in EVOH processability due to material embrittlement. Then, a small amount of montmorillonite (MMT) is mixed in the EVOH/DPE system: it results that for specific compositions MMT inhibits the DPE crystallization. At the same time, DPE, thanks to its high polarity and affinity with both clay and polymeric matrix, improves the intercalation of the nanoclays, promoting the penetration of the polymer chains within the layers of the clay. The synergistic effects of DPE and MMT in EVOH matrix is confirmed by DSC, WAXD, SAXS and TEM analyses. © 2015 Wiley Periodicals, Inc. J. Appl. Polym. Sci. **2015**, *132*, 42265.

KEYWORDS: clay; composites; packaging

Received 23 October 2014; accepted 19 March 2015
DOI: 10.1002/app.42265

INTRODUCTION

EVOHs, which are random copolymers containing ethylene and vinyl alcohol groups distributed along the chains, are widely used in food packaging and find useful applications as barrier resins, adhesives, compatibilizers, etc.[1] Indeed, these polymers are characterized by a high density of hydrogen bonds between the macromolecules, due to the presence of hydroxyl groups in an amount proportional to the vinyl alcohol content. The consequent high cohesive energy induces significant properties, for example excellent gas barrier performances, connected to a decrease in the available free volume for gas exchange.

Nevertheless EVOH could be quite troublesome when processed in multilayer structures. Among common issues it is worth to mention its limited thermal stability at the processing temperature typical of other widespread polyolefins and its decreasing stretchability at higher vinyl alcohol ratios. In fact, a high amount of OH groups in the backbone and therefore a high density of hydrogen bonds, which are positive for barrier performances to gases in a certain range of environmental humidity exposure, nevertheless cause an increment of stiffness of the EVOH items. This adds some difficulty to the preparation of oriented films or deep thermoforming of sheets. The issue is currently addressed by using more flexible EVOH grades, such as the ones rich in ethylene. The use of special terpolymers where a third monomer such as 3,4-dihydroxy-1-butene is introduced to the backbone[2] and blending EVOH with low crystallinity or amorphous polyamides (PA6-co-PA12 or PA6I,6T)[3,4] are also common practices. However, all the above-mentioned approaches produce a significant negative impact on barrier performances. Moreover, the achievement of a target value of permeability requires thicker structures than pure high vinyl alcohol EVOH grades. When compromises on oxygen permeability are not feasible, the authors found that the previous approaches invariably lead to increased costs and, in the case of polyamide blends, to a minor deterioration of optical properties.

Therefore, the addition of small molecular weight additives, rich in -OH groups, to EVOH can be a new approach to modify the final material properties. This strategy is described in a recent paper,[5] where N,N′- bis(2,2,6,6-tetramethyl-4-piperidyl)-isophthalamide (Nylostab SEED) is added to EVOH to create new macromolecular interactions: as a result, a decreased molecular mobility is generated, bringing increased stiffness and strength, increased overall deformability and a decrement in oxygen diffusion. By adopting the same approach, dipentaerythritol

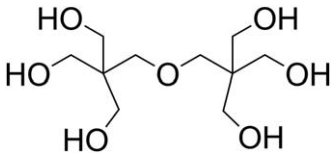

Figure 1. Chemical structure of DPE.

(DPE), whose chemical structure is reported in Figure 1, could be a perfectly suitable molecule to be used as a functional additive in EVOH and, in general, in polymers rich in hydroxyl groups. Indeed, DPE can strongly interact with polymers, inducing a high density of solid state hydrogen bonds, which can decrease EVOH crystallization rate from the melt and improve processability without affecting the good barrier performances.

Moreover, DPE has some further advantages: it is characterized by a low volatility and excellent heat and oxidation stability. Indeed, thanks to such features DPE is used in several applications: for example, its esters are suitable base oils for aviation gas turbine lubricants, high-temperature chain oil, high-temperature greases (for example, heat conduction greases).[6–8] DPE is also a component in some formulations in intumescent fire retardant (IFR) coatings,[9–11] such as an ammonium phosphates/DPE/melamine blend.

However, the high DPE crystallinity can lead to a phase separation in blend and to an unwanted deterioration of mechanical properties of the final polymeric blend. Indeed, it is important to underline that EVOH chains are known to be atactic[12] and, despite the lack of stereoregularity, they can crystallize at all copolymer compositions.[12,13] Most likely, it is due to the fact that the size of the hydroxyl groups on the polymer chains is small enough compared to the space available in the crystal structure so that the symmetry of the polymer is not significantly affected.

Therefore, EVOH and DPE crystallization processes are here investigated to understand the phase behaviour of the blends. Moreover, according to literature, that reports the synergistic effect of a polyol and montmorillonite (MMT) in some intumescent flame retardant systems,[14,15] new blends containing DPE and Dellite, not chemically modified MMT, were prepared and the synergistic effect of these two components on EVOH crystallization process was studied. A thermal and structural characterization of the new nanocomposites was carried out to comprehend the crystallization mechanisms of the final materials in view of their use in industrial processes, such as film manufacture.

EXPERIMENTAL

Materials

The blends prepared are based on a random copolymer of polyethylene and polyvinyl alcohol (EVOH32 - Kuraray EVAL F171B), which contains 32 mol % of polyethylene. This polymer will be referred to as EVOH in the text. Dipentaerythritol (DPE, Holtac™ D from Perstorp) and montmorillonite Dellite HPS (Laviosa, MMT, deriving from a naturally occurring especially purified montmorillonite, not chemically modified) were used as additives.

Mixing Procedure

Before blending, all the materials were oven-dried overnight at 120°C. The mixing was carried out in a twin-screw extruder Coperion ZSK-18, characterized by a temperature profile corresponding to 220–230°C. The feed rate was 2 kg h^{-1} and the screw speed 350 rpm.

Binary blends, as obtained by varying the ratios between EVOH and DPE, are listed in Table I. The samples are indicated with the code $EVOH_{XX}/DPE_{YY}$, where XX and YY are the weight percentage of EVOH and DPE, respectively. Blends which also contain MMT are described in Table II. Samples are called $EVOH_{XX}/DPE_{YY}/MMT_{ZZ}$ and $EVOH_{XX}/MMT_{ZZ}$, where ZZ indicates the weight percentage of MMT. The blends obtained by extrusion were compression moulded into films by applying heat and pressure in a press (Alfredo Carrea, Genova, Italy). The films were prepared by placing about 3.0 g of material between two metal plates positioned inside the press. The system was heated to about 30°C above melting temperature to completely melt the polymer. After heating, the films were left inside the press until they cooled to room temperature. Their thickness was about 0.5 mm.

Blend Characterization

The ^{1}H NMR analysis was carried out using a Varian Mercury 400 MHz spectrometer; the samples were initially dissolved in not deuterated hexafluoroisopropanol and then diluted with deuterated chloroform to have a final mixture in 80/20 volume ratio.

The calorimetric analysis was carried out by means of a Perkin-Elmer DSC6, calibrated with high purity standards. The measurements were performed under nitrogen flow. The thermal treatment consisted in a first heating scan to 240°C and 1 min of isotherm to erase the thermal history; a cooling scan from 240°C to 20°C at 10°C min^{-1} and 1 min of isotherm; finally, a second scan to 240°C at 10°C min^{-1}.

On the basis of the DSC thermograms, crystallization temperatures and enthalpies (T_c and ΔH_c) were determined in the cooling scan from the molten state; glass transition (T_g), melting temperatures and enthalpies (T_m and ΔH_m) were calculated from the second scan.

Wide angle X-ray diffraction (WAXD) patterns were recorded in the diffraction angular range 1.5–40° 2θ by a Philips X'Pert PRO diffractometer, working in the reflection geometry and equipped with a graphite monochromator on the diffracted beam (CuK_α radiation). Transmission patterns were recorded in the diffraction range 5–40° 2θ by a diffractometer GD 2000 (Ital Structures) working in a Seeman-Bohlin geometry and with a quartz crystal monochromator on the primary beam ($CuK_{\alpha 1}$ radiation).

Small angle X-ray scattering (SAXS) measurements were performed in a MBraun system by utilizing CuK_α radiation from a Philips PW1830 X-ray generator. The patterns were recorded by a position sensitive detector in the scattering angular range 0.1–5.0° 2θ and corrected for the blank scattering. A constant continuous background scattering[16] was subtracted and the obtained intensity values $\bar{I}(s)$ were smoothed, in the tail region, with the aid of the $s\bar{I}(s)$ versus $1/s^2$ plot.[17] Then Vonk's desmearing procedure[18] was applied and the one-dimensional

Table I. Composition and Thermal Data of EVOH, DPE, and Their Blends

Sample code	Composition EVOH/DPE (wt ratio)	T_c[a] (°C)	ΔH_c[a] (J g^{-1})	T_g[b] (°C)	T_m[b] (°C)	ΔH_m[b] (J g^{-1})
EVOH[c]	100/0	156	68	62	183	73
DPE	0/100	200	270	-	224	273
$EVOH_{95}/DPE_5$	95/5	153	60	55	180	64
$EVOH_{90}/DPE_{10}$	90/10	147	61	47	178	92
$EVOH_{88}/DPE_{12}$	88/12	100 + 145	7 + 56	47	178	88
$EVOH_{85}/DPE_{15}$	85/15	114 + 144	10 + 50	47	177	95
$EVOH_{77}/DPE_{23}$	77/23	131 + 141	96	n.d.	175 + 202	102

[a] Measured during the cooling scan from the melt.
[b] Measured during the second heating scan.
[c] Extruded EVOH sample.

scattering function was obtained using the Lorentz correction: $I_1(s)=4\pi s^2 I\ (s)$, where $I_1(s)$ is the one -dimensional scattering function and I(s) is the desmeared intensity function.

The sum of the average thicknesses of the crystalline and amorphous layers was determined as the Bragg identity period D of the function $I_1(s)$.

TEM analyses were performed by a FEI Technai G^2 (100 kV). Samples were microtomed by a LKB Ultrotom V. Sections about 80–100 nm thick were obtained and analysed.

RESULTS AND DISCUSSION

DSC and WAXD Analyses of Dipentaerythritol

Dipentaerythritol (DPE) is a molecule bearing many OH groups (Figure 1) and characterized by a high density (1.365 g cm^{-3}) and crystallinity. The calorimetric curves (Figure 2) show very intense and sharp melting and crystallization peaks. The crystallization and melting temperatures, measured during the cooling and second scans, respectively, are 200 and 224°C (see Table I). The corresponding enthalpies are 270 and 273 J g^{-1}, respectively, confirming a high degree of crystallinity. The WAXD pattern of DPE is reported in Figure 3: the angular positions of the most important reflections, to be found in the angular range of interest for EVOH, are indicated.

In addition, Figure 4 reports the WAXD spectra of the MMT sample (Dellite), used in this work.

Blends Between EVOH and DPE

Figure 5 shows the DSC thermograms (cooling and second scans) of EVOH and EVOH/DPE binary blends, with DPE percentage ranging from 5 to 23 wt %, while the corresponding data are reported in Table I. First of all, Table I highlights that T_g values change from 67°C in EVOH copolymer to 47°C in blends. As DPE can be considered responsible for hydrogen-bonding interactions with the EVOH macromolecular chains, the decrement of T_g could be due to a certain plasticizer effect of DPE, that tends to reduce the interactions between EVOH chains, increasing the distance between neighbouring chains. A similar effect is described in literature for EVOH in the presence of water molecules, which are easily incorporated into polymer supermolecular structures. This process decreases the polymer–polymer interactions, involving the weakening or breaking of hydrogen bonds between chains. Therefore, the increased chain mobility or flexibility in the amorphous state causes a notable decrement of T_g (from 60°C to 3°C for relative humidity varying from 0 to 100% for EVOH32).[1]

Figure 5 and Table I also point out that the crystallization temperature decreases with the increment of DPE amounts in the blends and the enthalpies come out sligthly lower than those expected. Therefore, the new hydrogen bonds between -OH groups of EVOH and DPE can disturb the crystallization process from the melt, inducing a notable reduction in Tc and a low level of crystallinity. The decrement in crystallinity was also

Table II. Composition of EVOH Blends Containing Montmorillonite

Sample code	Composition EVOH/ DPE/MMT (wt ratio)	EVOH/DPE (wt ratio)	DPE/MMT (wt ratio)
$EVOH_{72}/DPE_{21}/MMT_7$	72/21/7	77/23	75/25
$EVOH_{64}/DPE_{27}/MMT_9$	64/27/9	70/30	75/25
$EVOH_{53}/DPE_{35}/MMT_{12}$	53/35/12	60/40	75/25
$EVOH_{23}/DPE_{43}/MMT_{14}$	43/43/14	50/50	75/25
$EVOH_{74}/DPE_{22}/MMT_4$	74/22/4	77/23	83/17
$EVOH_{75}/DPE_{23}/MMT_2$	75/23/2	77/23	91/9
$EVOH_{96}$ /MMT_4	96/0/4	/	/
$EVOH_{93}$/ MMT_7	93/0/7	/	/
$EVOH_{91}$/ MMT_9	91/0/9	/	/

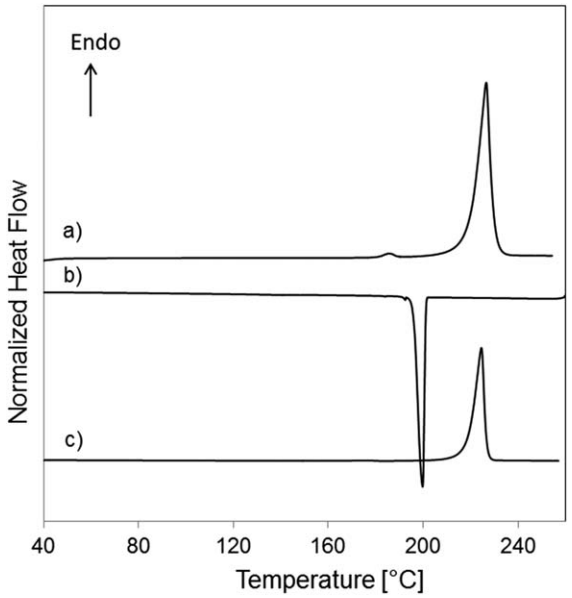

Figure 2. DSC curves of DPE: (a) first scan; (b) cooling scan; (c) second heating scan.

observed in the EVOH-Nylostab system and ascribed to the new interactions between polymer and additive.[5]

It is interesting to observe that, given a content of DPE equal or lower than 10 wt %, the blends are characterized by a single crystallization and melting process, due to the EVOH crystalline phase. On the other hand, a second crystallization process, with very low intensity and probably due to the DPE crystals, is also present in the samples containing 12 and 15 wt % of DPE. Finally, the $EVOH_{77}/DPE_{23}$ sample, containing 23 wt % of DPE, is characterized by two melting and crystallization processes, probably due to the presence of two crystalline phases. The sharp and intense crystallization peak at 131°C and the very high values of enthalpies suggest that DPE crystals are present in a large amount.

To confirm this hypothesis, the WAXD analysis was performed on films, prepared after extrusion. Thus, the thermal treatment that the films have undergone (melting and fast cooling), can be considered analogous to the melting and cooling processes

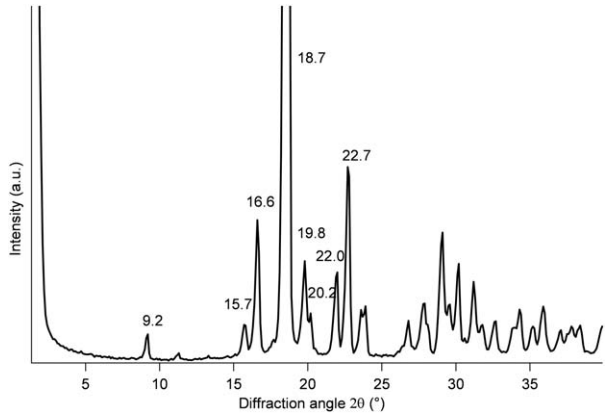

Figure 3. WAXD pattern of DPE.

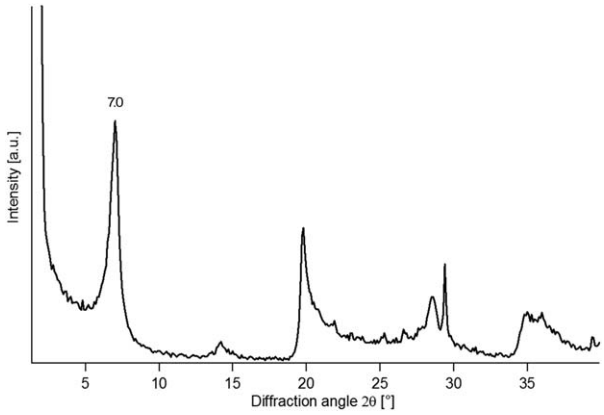

Figure 4. WAXD pattern of Dellite.

carried out in DSC. Therefore, the results of the WAXD analysis can be correlated to the DSC curves in the second scans.

Figure 6 shows some WAXD spectra of EVOH based films, containing different amounts of DPE and MMT. By focusing the attention on EVOH copolymer only, three types of crystalline systems have been identified in literature on the basis of on copolymer composition and crystallization conditions.[12,13,19] EVOH copolymers with vinyl alcohol contents of about 6–14 mol % were reported to crystallize in the orthorhombic crystal structure of PE, while those between 27 and 100 mol % crystallize in the monoclinic structure of PVOH. An intermediate hexagonal structure was observed at vinyl alcohol contents between 14 and 27 mol %. Moreover, the cooling rate can be adjusted to control not only the level of crystallinity, but also the crystal morphology of the polymer.

From Figure 6, it is evident that the film preparation by compression moulding induces the crystallization of EVOH in the monoclinic phase of PVOH. Indeed, the characteristic peaks at 19.6 and 20.3° 2θ are present. This is the expected crystalline phase for EVOH copolymer containing 32 mol % of PE units.[12,13,19] Moreover, considering the $EVOH_{77}/DPE_{23}$ blend, it is evident that the crystalline phase of PVOH is maintained, but also the peak at 18.7° 2θ, characteristic of DPE (Figure 3), is present. This peak is very intense and sharp, indicating a high level of crystallinity due to the additive and confirming that the crystallization of DPE is possible in the EVOH/DPE blends and two crystalline phases can coexist.

Therefore, it is possible to deduce from Figure 5 that the addition of DPE in EVOH matrix causes a lowering in the crystallization rate of EVOH, inducing a small decrement of the crystallization and melting temperatures, according to the DPE percentage. It is noteworthy that, when DPE is blended to EVOH up to 10 wt %, it does not crystallize, allowing the preparation of articles featuring enhanced flexibility, stretchability, and flowability without affecting optical properties (as observed during and after extrusion processes). On the other hand, DPE tends to crystallize when present in amounts over 10 wt % and creates a separate crystalline phase. Therefore, it should be interesting to try to increment the percentage of DPE, maintained in the amorphous state, in EVOH matrix. This aim is pursued using the addition of a third component, the MMT clay.

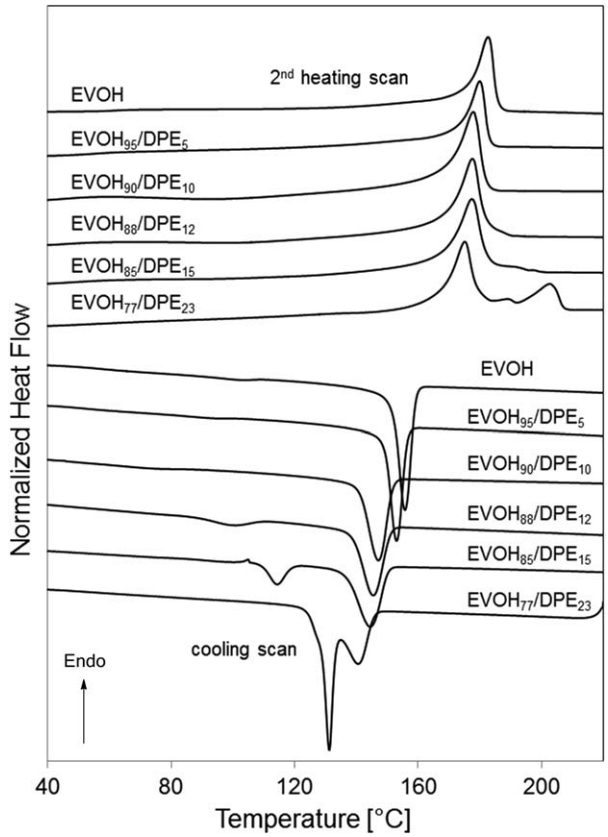

Figure 5. DSC curves of EVOH and its binary blends with DPE, prepared in extruder.

Blends Among EVOH, DPE, and MMT: Thermal Characterization

In Figure 7, the DSC scans of three significant samples are compared: EVOH, $EVOH_{77}/DPE_{23}$ and $EVOH_{72}/DPE_{21}/MMT_7$, which is a ternary blend containing 23% by weight of DPE with respect to EVOH. This means that the two blends here considered are characterized by the same EVOH/DPE ratio. The corresponding DSC data are reported in Table III.

First of all, it is notable that the T_g value of $EVOH_{72}/DPE_{21}/MMT_7$ sample is 48°C (Table III), i.e. significantly lower than

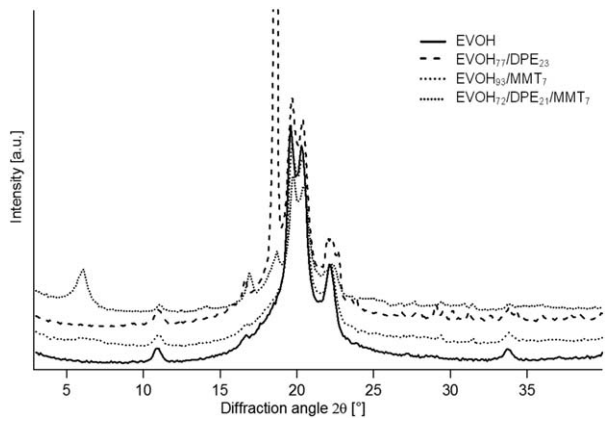

Figure 6. WAXD spectra of films containing different amounts of DPE and MMT.

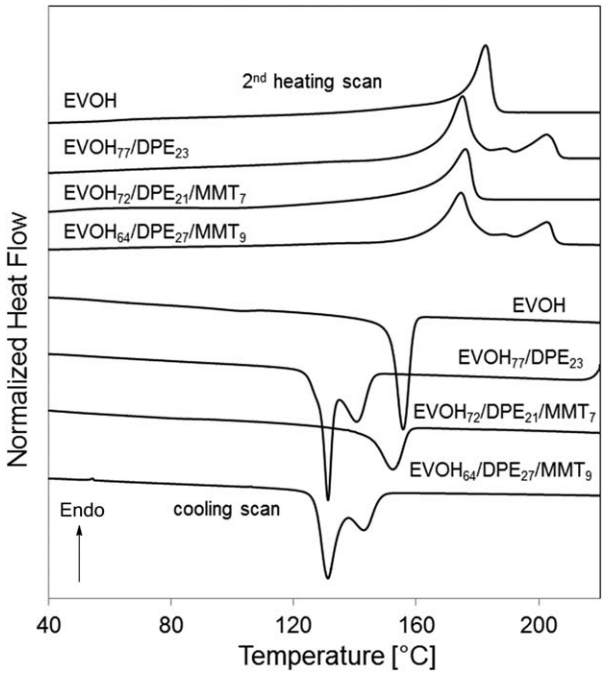

Figure 7. DSC thermograms of EVOH and some of its blends ($EVOH_{77}/DPE_{23}$, $EVOH_{72}/DPE_{21}/MMT_7$, $EVOH_{64}/DPE_{27}/MMT_9$).

that of EVOH copolymer (62°C) and similar to those of the blends in Table I (47°C). Therefore, as far as the amorphous phase is concerned, the presence of MMT does not modify the EVOH chain flexibility, due to the plasticization effect of DPE.

On the other hand, from Figure 7 it is notable that $EVOH_{77}/DPE_{23}$ and $EVOH_{72}/DPE_{21}/MMT_7$ samples are characterized by completely different thermal behaviours. Indeed, in the presence of montmorillonite the blend is characterized by a single crystallization and a single melting process. Therefore, it seems that DPE is no longer capable of crystallizing. Moreover, in $EVOH_{72}/DPE_{21}/MMT_7$ the crystallization process does not occur at such low temperatures as in $EVOH_{77}/DPE_{23}$ blend. In the presence of MMT, instead, crystallization takes place at temperatures slightly lower than those of EVOH, and the exothermal peak is wider and broader, indicating a crystallization process probably characterized by a slower rate with respect to the original polymer.

As to the crystalline phase, some further considerations are necessary. By observing all the WAXD spectra of Figure 6, first it is notable that the monocline phase of EVOH is always present, independently of the blend components. Moreover, the $EVOH_{93}/MMT_7$ sample does not show any peak at 18.7° 2θ. By comparing $EVOH_{77}/DPE_{23}$ and $EVOH_{72}/DPE_{21}/MMT_7$, it is notable that the peak at 18.7° 2θ is present also in the sample containing MMT, even though characterized by a very low intensity. Then, it is confirmed that in the presence of MMT, DPE crystallization is strongly hindered. It is important to highlight that the inhibition of DPE crystallization occurs in the sample where EVOH/DPE and DPE/MMT ratios are 77/23 and 75/25, respectively. This result is particularly significant. Indeed, the presence of a relatively high amount of DPE (23 wt % with

Table III. Thermal Data of EVOH32 Blends Containing Montmorillonite

Sample code	T_c[a] (°C)	ΔH_c[a] (J g^{-1})	T_g[b] (°C)	T_m[b] (°C)	ΔH_m[b] (J g^{-1})
$EVOH_{72}/DPE_{21}/MMT_7$	152	47	48	176	70
$EVOH_{64}/DPE_{27}/MMT_9$	131 + 143	91	n.d.[c]	174 + 203	93
$EVOH_{53}/DPE_{35}/MMT_{12}$	155 + 163	106	n.d.	171 + 211	114
$EVOH_{23}/DPE_{43}/MMT_{14}$	149 + 162 + 169	108	n.d.	171 + 214	16
$EVOH_{74}/DPE_{22}/MMT_4$	131 + 142	92	n.d.	175 + 203	98
$EVOH_{75}/DPE_{23}/MMT_2$	126 + 144	98	n.d.	175 + 203	102
$EVOH_{96}$ /MMT_4	153	57	59	181	64
$EVOH_{93}$/ MMT_7	155	58	58	180	63
$EVOH_{91}$/ MMT_9	154	58	58	181	66

[a] Measured during the cooling scan from the melt.
[b] Measured during the second heating scan.
[c] Not determined.

respect to EVOH) in the blend has positive effects in terms of EVOH processability, thanks to a reduction of EVOH crystallization temperature and crystallization rate. Moreover, in the blend, the negative effects due to the DPE crystallization, i.e. the material embrittlement, are avoided, thanks to the presence of MMT.

On the other hand, by increasing the relative amount of DPE with respect to EVOH ($EVOH_{64}/DPE_{27}/MMT_9$, where EVOH/DPE ratio is 70/30), the crystallization and melting processes of DPE take place, as shown by the double peaks reported in the DSC curves in Figure 7. By further increasing the relative amount of DPE in the blends ($EVOH_{53}/DPE_{35}/MMT_{12}$ and $EVOH_{23}/DPE_{43}/MMT_{14}$ samples, where EVOH/DPE ratios are 60/40 and 50/50, respectively, data in Table III), crystallization and melting processes are characterized by multiple peaks, with different and unusual shapes, indicating that some other phenomena probably take place. In any case, the presence of DPE crystals is recognizable. Finally, $EVOH_{74}/DPE_{22}/MMT_4$ and $EVOH_{75}/DPE_{23}/MMT_2$ samples are characterized by a lower MMT content with respect to DPE (DPE/MMT = 87/17 and 91/9, respectively), while the EVOH/DPE ratio is maintained equal to 77/23. The DSC curves, reported in Figure 8, highlight that multiple crystallization and melting processes are present. As they are attributable to the growth and melting of both EVOH and DPE crystals, it is evident that a small amount of MMT has a poor effect in inhibiting DPE crystallization.

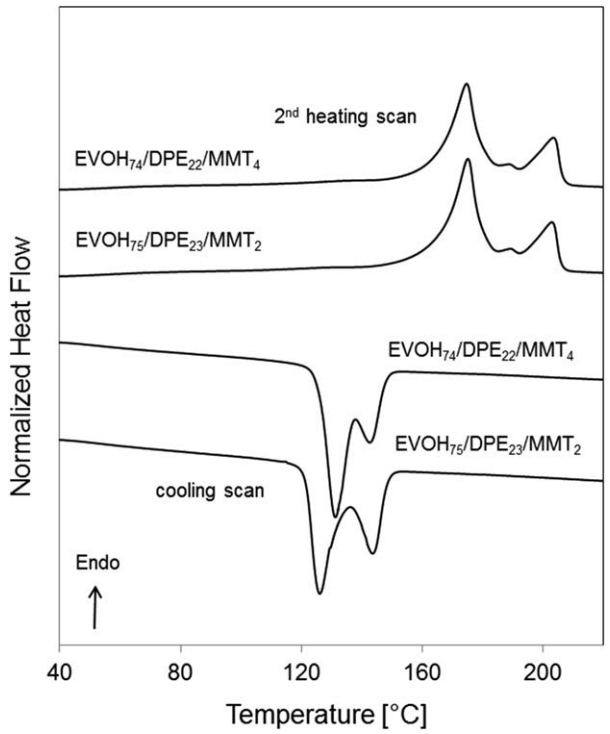

Figure 8. DSC curves of EVOH and some ternary blends at low MMT content.

Therefore, Dellite is able to hinder the DPE crystal growth only for specific blend compositions. Moreover, from Figure 9, which is a magnification of Figure 6, it is notable that the peak due to the clay is shifted from its original position at 7.0 (Figure 4) to 6.2 and 6.0° 2θ for $EVOH_{93}/MMT_7$ and $EVOH_{72}/DPE_{21}/MMT_7$, respectively. Therefore, the intercalation is successfully obtained, in particular in the presence of both DPE and MMT components. This means that the presence of DPE promotes the penetration of the polymer chains within the layers of the clay. This interesting result is probably due to the high polarity of DPE and its affinity with both clay and polymeric matrix. The result is also notable because the nanoclay is not chemically modified and, in general, its homogeneous dispersion in a polymeric matrix is not easily obtained.

Blends Among EVOH, DPE, and MMT: Morphological and Structural Characterization

To study more in depth the synergistic effects of DPE and MMT in ternary blends with EVOH, some further structural and morphological characterizations were carried out. Scherrer equation was applied to WAXD 001 reflection, associated with the portion of filler which remained stacked.[20] The equation allows us to estimate the thickness of crystallites on the basis of the full width at half maximum (β_0) of the corresponding WAXD peaks:

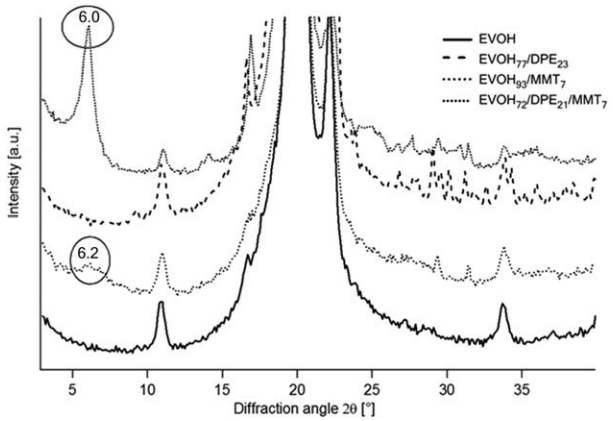

Figure 9. Magnification of WAXD spectra of films containing different amounts of DPE and MMT (clay peaks encircled).

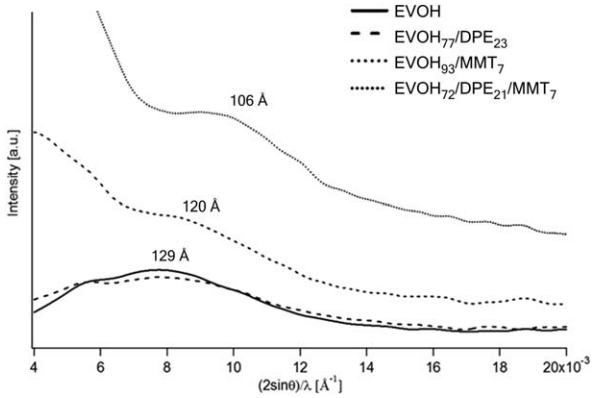

Figure 10. SAXS spectra of films containing different amounts of DPE and MMT.

$$L_{hkl} = \frac{K\lambda}{\beta_0 \cos\theta} \quad (1)$$

where L_{hkb} in this case L_{001}, represents the crystallite thickness in a direction perpendicular to that of the crystallographic plane identified by Miller indices *hkl*, $K = 0.91$ is a constant used in the case of smectites,[21] λ the wavelength of the X-radiation. Knowing L_{001} values, a further estimation on the number of layers forming clay stacks (tactoids) can be derived considering that

$$N = L_{001}/d_{001}, \quad (2)$$

where d_{001} is the d-spacing associated with the (001) basal signal of delight. Table IV reports the data obtained for MMT and EVOH binary and ternary blends. It is possible to deduce from such data that the average number of layers and the average size of tactoids in $EVOH_{72}/DPE_{21}/MMT_7$ are lower than in $EVOH_{93}/MMT_7$ and in Dellite, confirming that the simultaneous presence of DPE and MMT in EVOH matrix is very efficient in providing intercalated morphology. Small angle X-ray diffraction (SAXS), in the angular range corresponding to the lamellar morphology (Figure 10), can provide further morphological information on the films. Clay-related reflections, as recorded by SAXS, perfectly coincide with those already shown in Figure 8. It is possible to determine that the Long Period (sum of the crystalline and amorphous layer of lamellar stacks) remains the same (129 Å) for EVOH and $EVOH_{77}/DPE_{23}$. Therefore, DPE does not induce any change in the lamellar morphology. On the other hand, the addiction of Dellite ($EVOH_{93}/MMT_7$) causes a decrease of the Long Period (120 Å). Finally, the simultaneous presence of Dellite and DPE in $EVOH_{72}/DPE_{21}/MMT_7$, causes a synergistic effect: indeed, a further significant reduction of the Long Period (106 Å), corresponding to a change of the lamellar morphology, is observed.

Table IV. Number of Layers (*N*) Forming Clay Stacks along 001 Direction, Crystallite Thickness (*L*), and Diffraction Angle 2θ

Sample	L_{001} (Å)	$2\theta_{001}$	*N*
Dellite (MMT)	120	7.0	10
$EVOH_{93}/MMT_7$	80	6.2	6
$EVOH_{72}/DPE_{21}/MMT_7$	66	6.0	4

Finally, a TEM analysis was carried out to obtain more detailed information on the distribution of DPE and clay in the films. In Figure 11(a), it is possible to see the homogeneous morphology of EVOH, with amorphous and crystalline zones arranged randomly throughout the sample. For $EVOH_{77}/DPE_{23}$ [Figure 11(b)], the morphology is even more homogeneous: white regions are due to the "tearing" of the blade (during the cutting of the samples) due to areas of great rigidity. It is conceivable that these areas have a higher degree of crystallinity than the rest of the material and, thus, are rich in DPE. The black regions are probably due to folds formed during cutting which has caused plastic deformations.

In TEM images of $EVOH_{93}/MMT_7$, very compact aggregates of clay, that have not been dispersed homogeneously, are clearly visible [Figure 11(c)]. Figure 11(d) underlines the presence of smaller, compact, clay agglomerates that do not show any intercalation. The lack of crushing in smaller tactoids implies that the clay is not uniformly distributed in the material.

The simultaneous presence of DPE and clay in $EVOH_{72}/DPE_{21}/MMT_7$ leads to a morphology in which, although coarse aggregates of clay are still present, there is a better dispersion and fragmentation [Figure 11(e)]. In some cases it is possible to have intercalation [Figure 11(f)] as already observed by WAXD analysis (Figure 9).

Therefore, TEM images confirm the results of DSC and WAXD measurements. In $EVOH_{77}/DPE_{23}$, DPE is able to crystallize and creates a dishomogeneous morphology, with high rigidity zones. Moreover, in $EVOH_{93}/MMT_7$ a few small-sized fragments and many large clay agglomerates are evident. On the other hand, in $EVOH_{72}/DPE_{21}/MMT_7$, the crystallization of DPE does not occur; a homogeneous distribution of clay, with intercalation, has been observed. Therefore, the synergistic positive effect of DPE and MMT in improving the formation of a homogeneous morphology is confirmed by TEM observations, SAXS and WAXD analyses.

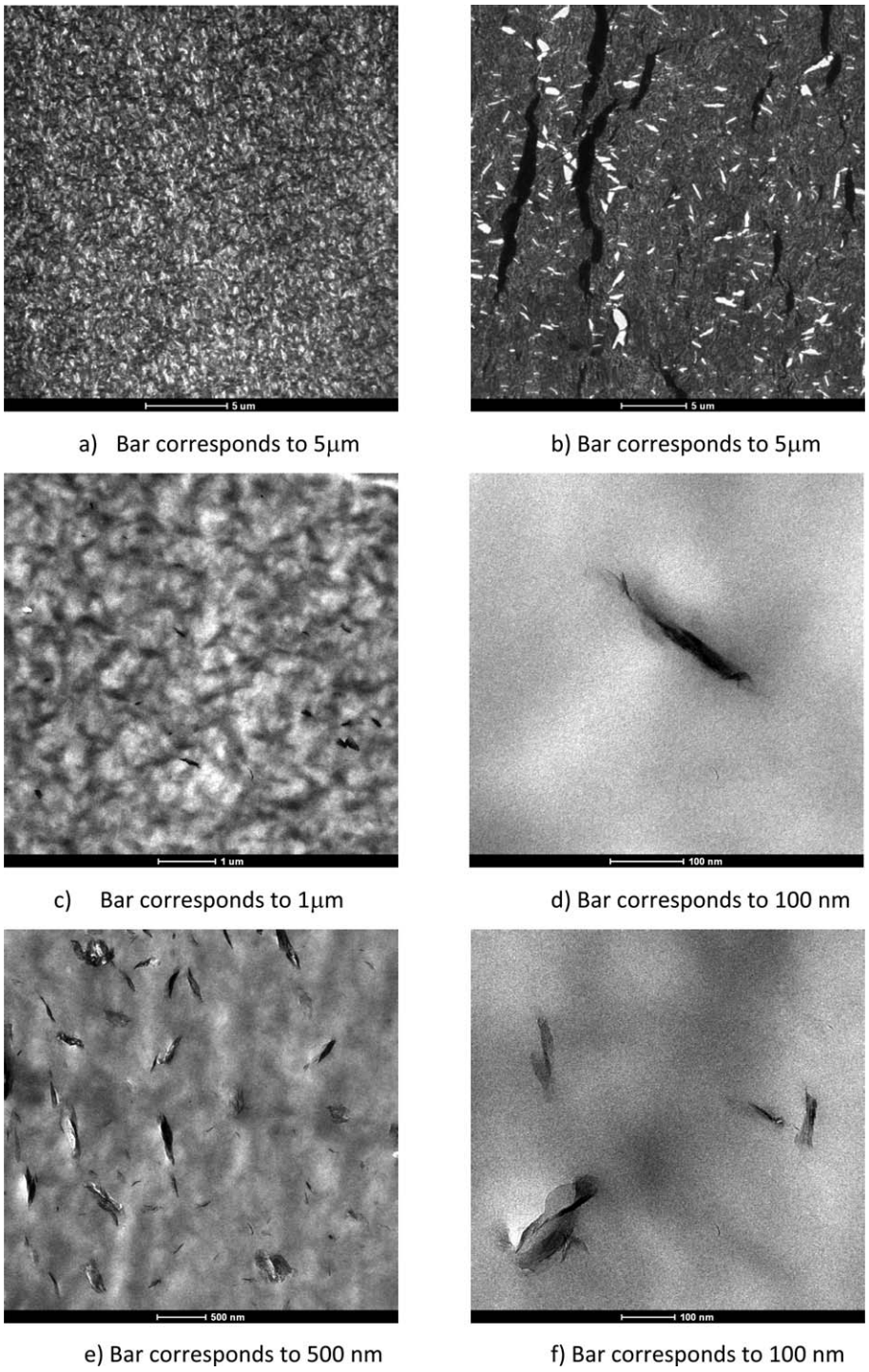

Figure 11. TEM images of (a) EVOH; (b) $EVOH_{77}/DPE_{23}$; (c) and (d) $EVOH_{93}/MMT_7$ at different magnifications; (e) and (f) $EVOH_{72}/DPE_{21}/MMT_7$ at different magnifications.

A final observation can be carried out by comparing transmission and reflection WAXD spectra. Indeed, the transmission WAXD analysis can provide information on the bulk of the material, while the reflection spectra are most affected by the surface. Figure 12 shows the transmission spectra, which can be compared with those reported in Figures 6 and 9. It is noteworthy that in the transmission WAXD patterns the reflections related to Dellite are totally absent for both $EVOH_{93}/MMT_7$ and $EVOH_{72}/DPE_{21}/MMT_7$.

This behaviour is completely different from that observed in the reflection spectra and is compatible with the hypothesis that the clay is preferentially located on the surface of the samples. Also this result can be highly significant to prepare materials with excellent barrier performances.

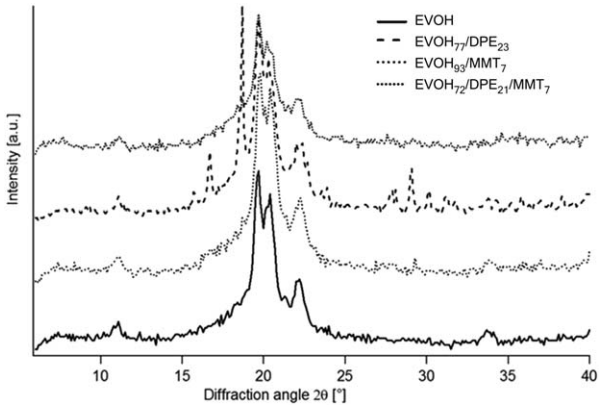

Figure 12. Transmission SAXS spectra of films containing different amounts of DPE and MMT

CONCLUSIONS

DPE is an interesting molecule, characterized by high number of -OH groups, which can contribute to create new morphologies in polar systems. In particular, when DPE is blended to EVOH it allows the preparation of articles featuring enhanced flexibility (lower values of T_g), enhanced stretchability, and flowability without affecting optical properties (observed during and after extrusion experiments). However, beyond a certain loading (above 10 wt %), DPE can crystallize and segregate during cooling, causing further problems in EVOH processability due to the general embrittlement of the material.

This phenomenon is fully prevented by the presence of MMT in the EVOH/DPE formulation. Indeed, Dellite, not chemically modified nanoclay, mixed in the EVOH polymeric matrix, inhibits the DPE segregation and crystallization tendency. For its part, DPE improves the intercalation of the nanoclays, promoting the penetration of the polymer chains within the layers of the clay. This interesting result is probably due to the high polarity of DPE and its affinity with both clay and polymeric matrix.

Therefore, EVOH blends, characterized by a well dispersion of additives, are easily obtained. These results are evident for specific relative amounts of DPE and MMT, that is, for the 77/23 EVOH/DPE and 75/25 DPE/MMT ratios.

WAXD, SAXS, and TEM analyses highlight the synergistic effects of the presence of both DPE and MTT in the polymeric matrix. Indeed, the simultaneous addition of the nanoclay and the polyol induces changes in lamellar morphology, with a significant reduction of the Long Period (sum of the crystalline and amorphous layer of lamellar stacks); the average number of layers in tactoids has a notable decrement. From TEM observations, a homogeneous distribution of clay, with intercalation, can be more easily observed.

We do believe that the results arising from this work can be extended beyond the possible technological interest in film manufacture. The easy preparation of well dispersed and concentrate formulations of MMT, DPE, and EVOH can be a practical approach for the preparation of various masterbaches suitable for other polar polymers (e.g., polyamides).

Vis-a-vis these interesting results, it is possible to hypothesize that also in other blends between DPE and MMT (for example, in intumescent formulations to prepare flame resistant materials), the positive relationship between the two components can cause beneficial effects on the realization of homogeneous morphologies and more effective systems.

ACKNOWLEDGMENTS

Financial support from Tetra Pak (Suisse) SA is gratefully acknowledged.

REFERENCES

1. Mokwena, K. K.; Tang, J. *Crit. Rev. Food Sci.* **2012**, *52*, 640.
2. Moriyama, T.; Inoue, K. *Eur. Pat. Appl.* EP1801154A1 (**2007**).
3. Schroeder, G. O.; Newsome, D. L.; Haffner, W. B. US Pat. 4,828,915 (**1989**).
4. Deak, G. I.; Jones, A. *J. Eur. Pat. Appl.* EP305146A1 (**1988**).
5. Péter, Zs.; Kenyó, Cs.; Renner, K.; Kröhnke, Ch.; Pukánszky, B. *Express Polym. Lett.* **2014**, *8*, 756.
6. García, J.; Naccoul, R. A.; Fernandez, J.; Razzouk, A.; Mokbel, I. *Ind. Eng. Chem. Res.* **2011**, *50*, 4231.
7. Zhang, L.; Cai, G.; Wang, Y.; Eli, W. *Lubr. Sci.* **2013**, *25*, 329.
8. Paredes, X.; Pensado, A. S.; Comuñas, M. J. P.; Fernánd, J. *J. Chem. Eng. Data* **2010**, *55*, 3216.
9. Zhang, S.; Horrocks, A. R. *Prog. Polym. Sci.* **2003**, *28*, 1517.
10. Lv, P.; Wang, Z.; Hu, K.; Fan, W. *Polym. Degrad. Stab.* **2005**, *90*, 523.
11. Gu, J.-W.; Zhang, G.-C.; Dong, S.-L.; Zhang, Q.-Y.; Kong, J. *Surf. Coat. Technol.* **2007**, *201*, 7835.
12. Takahashi, M.; Tashiro, K.; Amiya, S. *Macromolecules* **1999**, *32*, 5860.
13. Cerrada, M. L.; Pérez, E.; Perena, J. M.; Benavente, R. *Macromolecules* **1998**, *31*, 2559.
14. Tang, Y.; Hu, Y.; Li, B.; Liu, L.; Wang, Z.; Chen, Z.; Fan, W. *J. Polym. Sci. Part A: Polym. Chem.* **2004**, *42*, 6163.
15. Tang, Y.; Hu, Y.; Wang, S.; Gui, Z.; Chen, Z.; Fan, W. *Polym. Int.* **2003**, *52*, 1396.
16. Vonk, C. G.; Pijpers, A. P. *J. Polym. Sci. Polym. Phys. Ed.* **1985**, *23*, 2517.
17. Vonk, C. G. *J. Appl. Crystallogr.* **1973**, *6*, 81.
18. Vonk, C. G. *J. Appl. Crystallogr.* **1971**, *4*, 340.
19. Zhang, Q.; Lin, W.; Chen, Q.; Yang, G. *Macromolecules* **2000**, *33*, 8904.
20. Klug, H. P.; Alexander, L. E. X-ray Diffraction Procedures: For Polycrystalline and Amorphous Materials, 2nd ed.; Wiley: New York, **1974**.
21. Brindley, G. W.; Brown, G. Crystal Structures of Clay Minerals and Their X-ray Identification. Mineralogical Society: London, **1980**.